Small-Scale Sea Surface Temperature Structure

JAMES J. SIMPSON[1] AND CLAYTON A. PAULSON

School of Oceanography, Oregon State University, Corvallis, 97331

(Manuscript received 4 September 1978, in final form 5 October 1979)

ABSTRACT

Observations of sea surface temperature and wave height were made from a large, manned spar buoy (R/P *FLIP*) ~100 km off the coast of Baja California. Surface temperature was measured with a radiation thermometer which viewed a disc on the surface 12 cm in diameter. The instrument responded to frequencies up to 3 Hz. Wave height was measured with a resistance gage located close to the field of view of the radiometer.

Log-log plots of spectra of sea surface temperature exhibit a plateau between 0.05 and 0.5 Hz, followed by a rapid decrease in energy at frequencies > 1 Hz. A coherence of 0.5 between waves and surface temperature occurs at the same frequency as the peak in the wave spectrum. Phase spectra show that warm temperatures associated with the thinning of the surface viscous layer occur systematically upwind of the crests of the dominant gravity waves and downwind of the crests of steeply sloping, shorter period gravity waves. The warm temperatures are hypothesized to be caused by enhanced wind stress upwind from the crests and by surface instability and surface convergence downwind from the crests.

The magnitude of the mean temperature difference between the surface and the warmer, well-mixed water below is estimated from the surface temperature record. It is assumed that the warmest surface temperatures observed are associated with thinning of the viscous layer and are representative of the well-mixed water below. The dimensionless constant in a formula due to Saunders (1967), which relates the temperature difference to wind stress and heat flux, is found to be seven.

1. Introduction

With the improvement of radiometric techniques, it became possible to investigate the surface or "skin" temperature of the sea. Ball (1954), Ewing and McAlister (1960), McAlister (1964) and McAlister and McLeish (1969) were among the first to make radiometric measurements of sea surface temperature which demonstrated that the surface is typically a few tenths of a degree Celsius cooler than the temperature some tens of centimeters below. Earlier measurements by other methods (e.g. Woodcock, 1941) also demonstrated that the upper few millimeters of natural water surfaces were typically cooler than the water below. The temperature difference occurs because the vertical flux of heat Q just below the surface is generally upward, the total being the sum of the fluxes to the atmosphere of net longwave radiation R, sensible heat H, and latent heat E, i.e., $Q = H + E + R$.

A schematic diagram of the upper centimeter of the sea is shown in Fig. 1. Just below the interface there is a viscous sublayer of thickness δ in which the transfer of heat and momentum is primarily by molecular processes, from which it follows that the vertical temperature gradient is approximately constant. Below the viscous sublayer, turbulent mixing dominates and the temperature gradient is small.

Saunders (1967), on the basis of dimensional arguments, suggested that the difference between the surface temperature T_s and the well-mixed bulk temperature T_b below the surface is given by

$$T_b - T_s = \frac{\lambda \nu Q}{k(\tau/\rho)^{1/2}}, \qquad (1)$$

where λ is a dimensionless constant, ν the kinematic viscosity of water, k the thermal conductivity, τ the wind stress and ρ the density of water. Saunders suggested that the value of λ would lie between 5 and 10.

Hasse (1971) and Deacon (1977) have derived expressions similar to (1), but containing no arbitrary constants, derived from models of the viscous sublayer based on laboratory observations of flow near a solid boundary. Hasse (1971) found good agreement between his model and observations in which the surface temperature was determined by extrapolation of nearly adiabatic atmospheric temperature profiles to the surface. Hasse's observations are in good agreement with (1) when $\lambda = 8$ as shown by Paulson and Parker (1972). For a temperature of 20°C, Deacon's model is similar to (1) with $\lambda = 8.2$. For observations in the laboratory, λ ranges from 4

[1] Present affiliation: Scripps Institution of Oceanography, La Jolla, CA 92093.

0022-3670/80/030399-12$07.00

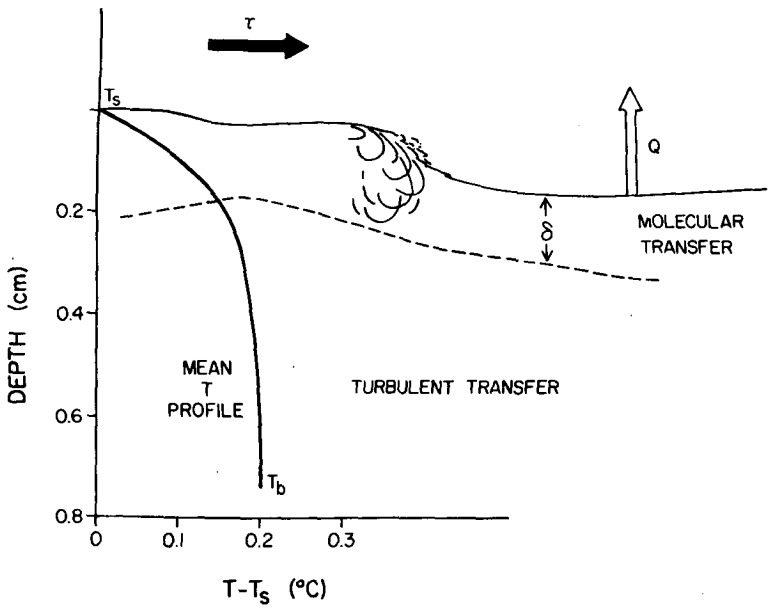

FIG. 1. Schematic diagram showing the processes affecting the temperature profile in the upper ocean. Here τ is the wind stress, Q the upward heat flux from just below the surface, δ the thickness of the viscous sublayer, T_s the mean surface temperature and T_b the mean temperature at a depth below 1 cm.

to 15, depending on whether or not waves are present (Hill, 1972; Paulson and Parker, 1972).

Radiometric observations of the sea surface temperature show temperature variations of a few tenths of a degree Celsius. The variability on small time scales (1–5 s) might be caused by the thinning or destruction of the viscous sublayer by the action of one of several possible mechanisms: 1) locally intense turbulence within the water, perhaps associated with a breaking wave; 2) a wind gust acting on the surface, causing a local increase in stress; or 3) the presence of waves. The occurrence of warm spikes in the temperature record particularly suggests the momentary destruction or thinning of the viscous sublayer.

Witting (1971) suggested on theoretical grounds that for an assumed constant heat flux, the presence of capillary waves could reduce $T_b - T_s$ by as much as a factor of 9 in comparison to the undisturbed case. Witting also suggested gravity waves would be an order of magnitude less effective and that the maximum in the temperature should lead the wave maximum by 45°.

Miller and Street (1978) recently reported a laboratory investigation of surface temperature fluctuations associated with waves. Waves were mechanically driven and various wind speeds and air-water temperature differences were imposed. The magnitude of the surface temperature variations was between 10 and 100% of $T_b - T_s$, in qualitative agreement with Witting (1971). For light winds, the peak of the temperature wave occurred on the leeward side of the mechanically generated surface wave. For moderate to high winds, the trough of the temperature wave occurred on the leeward side. A satisfactory explanation for this behavior is lacking. The extent to which Miller and Street's results can be generalized for the open sea is uncertain.

The objective of this paper is to describe radiometric observations of the sea surface temperature made simultaneous to measurements of wave height and surface fluxes. Insight is sought into the physical processes associated with variability in surface temperature.

2. Observations

Observations of sea surface temperature and wave height were made from the R/P *FLIP* [Floating Instrument Platform, (Bronson and Glosten, 1968)] approximately 60 mi off the coast of Baja California during the period 23–28 March 1973. The *FLIP* is a large manned spar buoy with ~90 m of its 110 m length submerged, resulting in a high degree of stability. Typical heave amplitudes were ~10 cm, while pitch and roll amplitudes were usually less than 2°. The *FLIP* drifted freely during the experiment, generally toward the southeast, with positions ranging from 31°28′N, 118°17′W at the beginning of the experiment to 30°48′N, 117°35′W at the end.

Sea surface temperature was measured with a Barnes Engineering Co. PRT-5 radiation thermometer responding to radiation with wavelengths in the range 8–14 μm. The half-power field of view of the

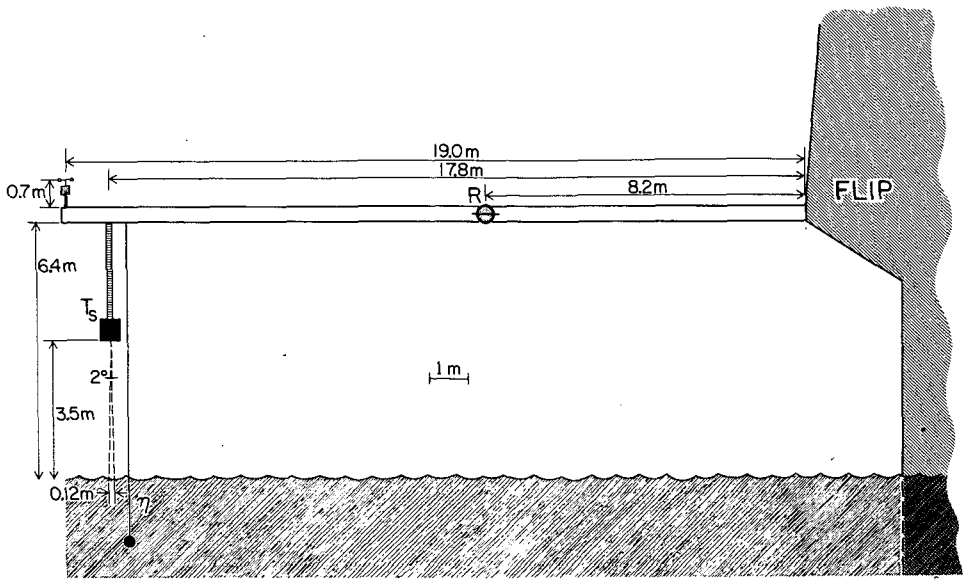

FIG. 2. Diagram showing the locations of instruments used to measure the sea surface temperature T_s, the wave height η, the wind speed U, and the net longwave radiative flux R. The diameter of *FLIP* at the surface is 4.2 m.

instrument is 2°. The instrument was mounted on the port boom of the *FLIP*, 18 m from the hull and 3.5 m above mean sea level, as shown schematically in Fig. 2. The *FLIP* naturally aligned itself with respect to the wind such that the boom extended perpendicular to the wind direction. The spot on the surface viewed by the instrument had a diameter of 12 cm (corresponding to the diameter at which the response has dropped to 50% of maximum). The instrument was operated with a low-pass filter on the output set at 3 Hz. The sensitivity of the instrument is ~0.03°C and the absolute accuracy is 0.5°C. Errors in the measurement of T_s caused by the reflection of longwave radiation from the *FLIP* are shown to be negligible in the Appendix.

Wave height η was measured with a resistance gage using nichrome wire having a diameter of 0.125 mm. The wire was suspended from the port boom of the *FLIP* as close to the radiation thermometer as practically possible. The wire was weighted with lead to keep its orientation near vertical. The resistance of the wire was measured before and after the experiment to insure that no change in resistance occurred because of stretching. The frequency response and sensitivity of the wave gage was limited by the effects of surface tension to about 3 Hz and 4 mm, respectively.

Wind speed was measured with a cup anemometer located near the end of the boom, as shown in Fig. 2. Dry-bulb and wet-bulb temperatures were measured approximately hourly by use of a ventilated psychrometer at a height of ~10 m above mean sea level. Bucket temperatures were recorded at the same time. Estimates of τ, H and E were obtained by use of the standard bulk formula. The exchange coefficient employed was 1.4×10^{-3}. Net longwave radiation was measured with a C. A. Thornthwaite Associates net radiometer. All of the reported observations were at night, thereby eliminating any possible complications caused by absorption of solar radiation in the upper millimeters. A summary of the conditions during each run is given in Table 1.

Data were recorded in analog form on magnetic tape. The signals were monitored simultaneous to recording on a strip-chart recorder. Examples of the data are shown in Fig. 3. The records show the occurrence of warm spikes of temperature having a magnitude of 0.3°C, often associated with a steep part of the wave profile. Apart from the spikes, there are fluctuations in temperature over a broad range of frequencies with peak-to-peak amplitudes on the order of 0.1°C.

3. Analysis

Following the experiment, the surface temperature and wave height signals were low-pass filtered at 10 Hz and digitized at a rate of 20 samples per second. Blocks of 16 384 data points, corresponding to 13.6 min of observations, were then constructed. Each run consisted of from four to six contiguous blocks.

A spectral analysis was carried out on both the surface temperature and the wave record. Fourier coefficients were computed for each of the blocks. The coefficients were combined to obtain the spectral energy densities, ϕ_T and ϕ_η, the cospectrum

TABLE 1. Summary of measurements and statistics, including mean wind speed $\bar{U}$, surface drift speed U_s, wind stress τ, flux of latent heat E, flux of sensible heat H, net longwave radiative flux R, upward heat flux just below the surface Q, fractional cloud cover C, rms wave height σ_η, mean surface temperature $\bar{T}_s$, rms sea surface temperature σ_{T_s}, mean difference between bulk oceanic temperature and surface temperature $\overline{\Delta T}$, the constant λ in Saunders' (1967) formula, and the symbol key used to identify individual runs in the composite spectra of Figs. 5, 8 and 9.

Run no.	Date (March 1973)	Time begin	$\bar{U}$ (m s^{-1})	U_s (m s^{-1})	τ (Pa)	E ←	H (W m^{-2})	R	Q →	C (tenths)	σ_η (m)	$\bar{T}_s$ ←	σ_{T_s} (°C)	$\overline{\Delta T}$ →	λ	Symbol key
2	23	1928	8.2	0.05	0.116	117	14	68	199	4	0.69	14.8	0.05	0.29	8	●
3	23	2115	7.7	0.05	0.102	108	10	51	168	5	0.67	15.3	0.06	0.29	9	○
4	23	2303	8.5	0.18	0.125	124	17	60	201	4	0.70	15.2	0.07	0.29	8	▲
7	24	0418	5.5	0.12	0.052	124	17	37	178	6	0.42	15.3	0.10	0.26	5	△
10	24	1941	7.1		0.087	124	2	22	148		0.40	14.9	0.08	0.19	6	■
11	24	2127	6.7		0.077	99	2	18	119		0.61	15.4	0.08	0.16	6	□
12	24	2314	7.1	0.05	0.087	115	4	58	177	2	0.60	15.1	0.07	0.28	8	◆
14	25	0234	5.6	0.08	0.054	92	7	34	133	9	0.42	14.8	0.10	0.24	7	◇
29	26	2002	9.2	0.25	0.146	155	12	55	222	0	0.56	15.0	0.05	0.27	8	×
31	26	2325	7.0	0.22	0.085	113	9	32	154	9	0.60	15.1	0.09	0.26	8	⊙

$C_{\eta,T}$, and the quadrature spectrum $Q_{\eta,T}$. These spectra were averaged over non-overlapping frequency bands equally spaced on a logarithmic scale to obtain smoothed spectral estimates. Coherence and phase spectra ($\gamma_{\eta,T}$ and $\theta_{\eta,T}$, respectively) were calculated from the smoothed spectral estimates by use of

$$\gamma_{\eta,T} = [(C^2_{\eta,T} + Q^2_{\eta,T})/\phi_\eta\phi_T]^{1/2},$$

$$\theta_{\eta,T} = \tan^{-1}(Q_{\eta,T}/C_{\eta,T}).$$

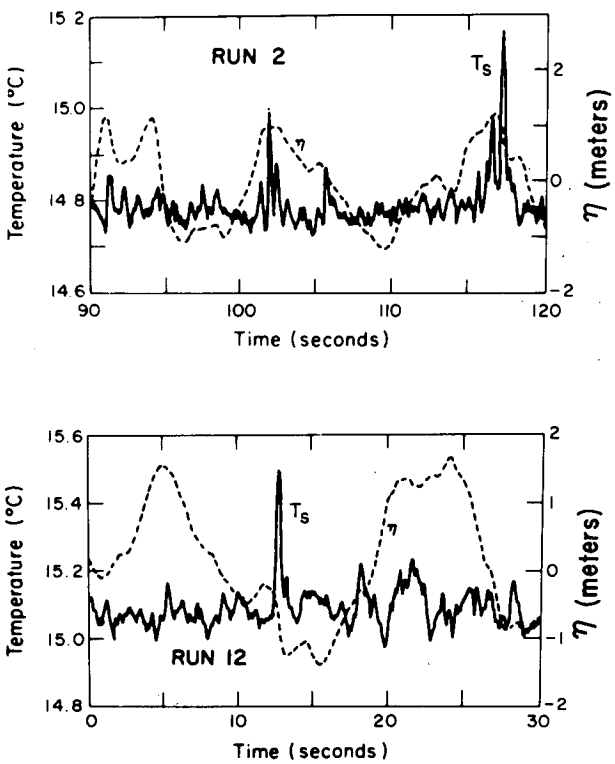

FIG. 3. Simultaneous measurements of sea surface temperature (T_s) and wave height (η) illustrating the occurrence of warm spikes.

Then the smoothed spectral energy density, coherence and phase spectra were averaged over blocks.

Confidence intervals for the energy density were calculated using a chi-square random variable with n equivalent degrees of freedom. Within a given frequency band, the equivalent degrees of freedom $n(f)$ is defined as twice the square of the block and band-averaged spectral estimate divided by the estimated variance of the sample average associated with the estimate, i.e.,

$$n(f) = \overline{2\phi(f)}^2/\mathrm{var}[\phi(f)].$$

Confidence intervals so constructed reflect the measured spectral variability within a given block-averaged frequency band.

Confidence intervals for the coherence were calculated using the procedure of Bendat and Piersol (1971). Additionally, a 95% significance level for the coherence was calculated using the procedure of Panofsky and Brier (1958) in which the limiting coherence β at probability level p is given by $\beta = [1 - p^{\{1/[(df/2)-1]\}}]^{1/2}$. As pointed out by Julian (1974) the appropriate number of degrees of freedom (df), is not the Blackman and Tukey (1958) definition but rather the effective number of Fourier components in the spectral window, i.e., df/2. This relation compares the limiting coherence and the measured coherence for a given probability level on the null hypothesis of zero population coherence (Julian, 1974) and agrees to within three decimal places with values obtained by following the procedures of Amos and Koopmans (1963). For the limit of large N, β approaches zero as expected. Confidence intervals for the phase estimates were determined using procedures suggested by Jenkins and Watt (1968).

Since the wave spectrum falls off approximately as ω^{-5}, it was necessary to consider the possible effects of spectral leakage on estimates of the vector

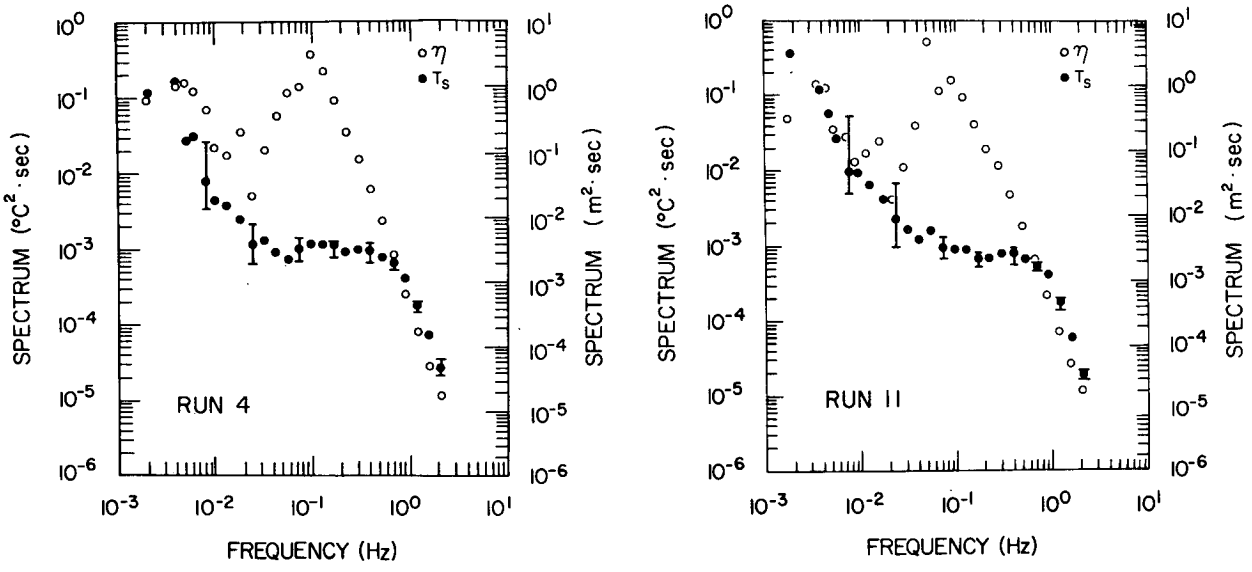

FIG. 4. Representative spectra of sea surface temperature (closed circles) and wave height (open circles). The vertical bars are the 95% chi-square confidence intervals.

coherence. For this purpose the data were partially prewhitened by calculating first differences. Differentiation is expected to reduce the slope of the spectrum of waves from ω^{-5} to ω^{-3} and hence is a good signal preconditioner with which to investigate the possible effects of spectral leakage. The resulting time series was Fourier-transformed as above. Coherence spectra for both (η,T_s) and $(\Delta\eta,T_s)$ for a typical run are shown in Fig. 6. The figure clearly shows that there is no significant difference between the two coherence spectra. A similar analysis was performed on most of the runs in Table 1 and the results were the same. These results indicate that spectral leakage did not affect the computation of the coherence spectra. Phase spectra for the same two cases are shown in Fig. 7. Where the coherence is high, the two phase spectra are similar. As higher frequencies are approached, the phase between surface temperature and differenced wave height becomes random at lower frequencies than the phase between surface temperature and wave height. This behavior may be caused by noise introduced by differencing the wave signal. In any case, the general behavior of the two spectra is consistent.

Estimates of spectral leakage can also be made on purely theoretical grounds by considering the effects of window shape and series length on the Fourier-transformed data. The data series was windowed with a boxcar window. The Fourier transform of the boxcar window has the form (Cooley *et al.*, 1967)

$$h(\omega) = \frac{1}{2\pi N}\left[\frac{\sin(N\omega\Delta t/2)}{\sin(\omega\Delta t/2)}\right]^2,$$

where N is the number of data points in a block and Δt the sampling interval. Leakage can only affect the spectral estimates when the ratio of side-lobe to central-peak energy is large. However, from the analytical form of $h(\omega)$, it is easy to see that as $N \to \infty$, the width of the frequency range with considerable spectral energy in the side lobes of the $h(\omega)$ window approaches zero. For the analysis presented in this paper, the length of the blocks (16 384 data points) used in the computations minimized the effects of leakage.

4. Spectra

Representative spectra of sea surface temperature and wave height are shown in Fig. 4. The shape of the spectra of wave height is similar for all of the runs, with peaks in the wave spectra occurring at frequencies between 0.055 and 0.097 Hz. Swell was negligible during most of the runs and the waves were taken to be wind-driven, traveling slower than the wind. The magnitude of the spectra at the peak ranged from 1.0 to 5.1 m² s. The standard deviation of wave height and surface temperature is given in Table 1 for each of the runs.

As shown in Fig. 5, the individual spectra of surface temperature are all similar to the examples shown in Fig. 4, both in shape and in magnitude. A peak occurs at low frequencies and, as frequency increases, spectral energy declines to a plateau between 0.05 and 0.5 Hz, followed by a rapid decrease in energy for frequencies above 1 Hz. There is often a small peak at the same frequency as the peak in the wave spectrum.

The spectra at low frequencies may be spurious because, as has been suggested by Saunders (1970), the variation of sky temperature associated with variations in cloud cover and type can cause non-

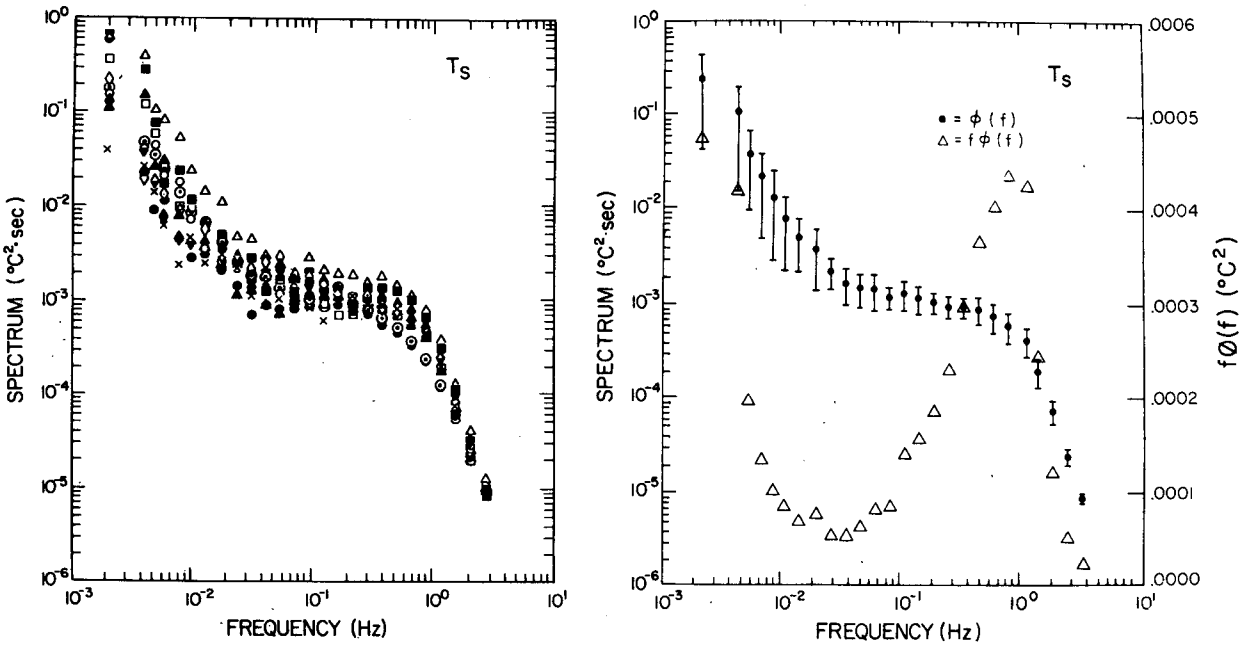

FIG. 5. Unaveraged and averaged spectra of sea surface temperature versus frequency. The symbols are defined in Table 1. The triangles in the figure represent the average spectrum of $f\phi(f)$ vs f, where f is frequency (Hz).

negligible, fictitious fluctuations in measured temperature. These fictitious fluctuations are caused by the reflection of longwave radiation from the surface. Even though the reflectivity is small (0.02), variation in sky temperature may cause erroneous fluctuations in observed temperature of several tenths of a degree Celsius (Saunders, 1970). Even under clear skies, variations in humidity and air temperature may cause variations in downward longwave radiation which would in turn cause spurious observed fluctuations in surface temperature. The likelihood of errors in the low-frequency fluctuations is supported by examination of time series of observations of surface temperature and net upward longwave radiation which reveal a negative correlation for periods longer than a few minutes. If the fluctuations were caused by fluctuations of surface temperature, the correlation would be positive. The magnitudes of the low-frequency fluctuations of observed T_s and R are on the order of 0.3°C and 2 mW cm^{-2} peak to peak, during periods of partial cloudiness. However, even during run 29 for which skies were reported to be clear, there were negatively correlated low-frequency fluctuations of T_s and R for about half the run. Conditions may not have been totally clear during this run because observations of cloudiness are difficult to make at night.

On the basis of the foregoing discussion, we conclude that observed fluctuations of T_s for periods greater than a few minutes may be in error. The magnitudes of the spectral estimates of T_s shown in Fig. 5 may therefore be too large for frequencies below 0.01 Hz.

Interpretation of the spectra of sea surface temperature at higher frequencies is complicated because temporal changes cannot be ignored and advection by surface waves is not steady. Attempts were made to nondimensionalize the spectra of sea surface temperature (Fig. 5) in hopes of establishing a universal form. In one of the attempts, the right side of Eq. (1) was used as a temperature scale. The attempts at nondimensionalization all failed to significantly reduce the scatter in the observations.

Representative coherence spectra computed for wave height and surface temperature are shown in Fig. 6. In both runs 4 and 11 there is a peak at the frequency at which the peak in the wave spectrum occurs, 0.097 and 0.055 Hz, respectively. The peak is characteristic of all of the runs.

The large values of coherence at frequencies ~0.01 Hz shown in Fig. 6 are spurious. They are due to the low-frequency motions of *FLIP*. Vertical motions at the location of the wave gage cause an erroneous fluctuation in wave height, while pitch and roll cause fluctuations in measured surface temperature as the radiation thermometer scans along the surface in the presence of a horizontal temperature gradient. The vertical motion is inevitably correlated with rolling motions of *FLIP*, giving rise to the observed coherence.

The question arises whether the low-frequency motions of *FLIP* have caused significant error in

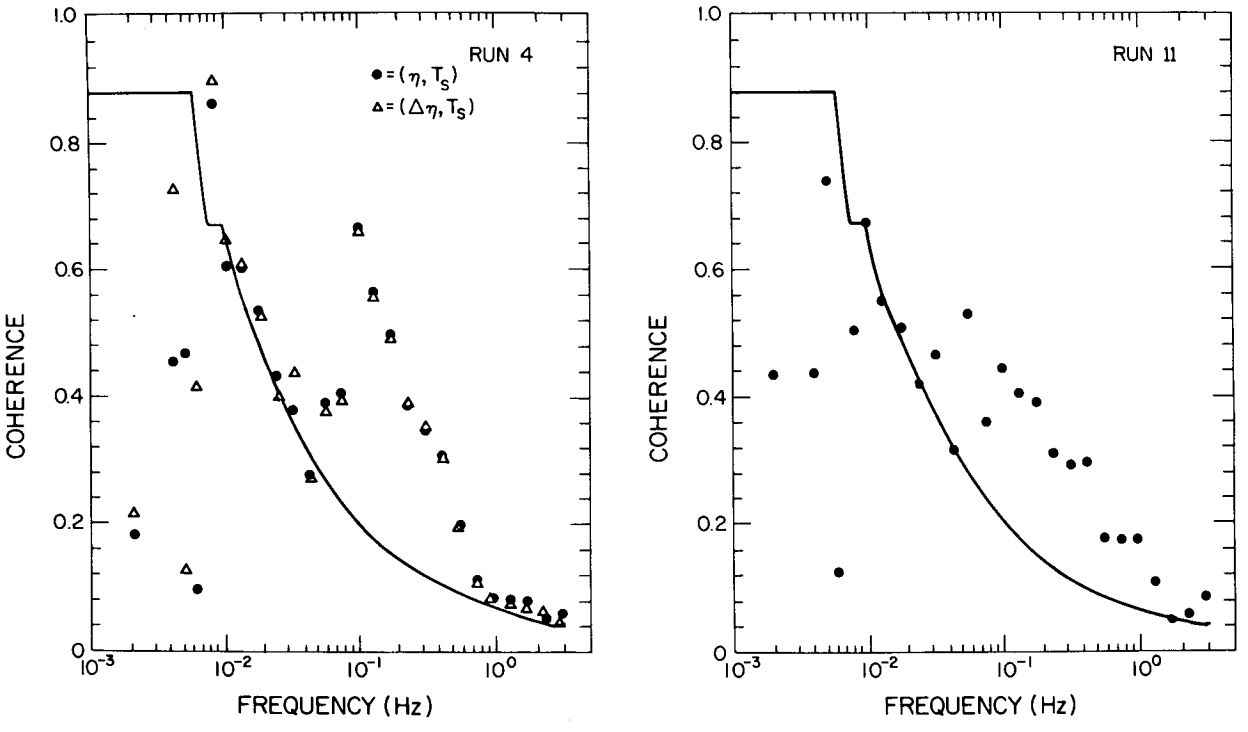

FIG. 6. Representative coherence spectra for sea surface temperature and wave height (circles). The line is the 95% significance level. The corresponding coherence spectrum (run 4) for sea surface temperature and first differenced wave height ($\Delta\eta$) is shown by the triangles.

the low-frequency spectra of sea surface temperature. Taking 1° as the typical pitch amplitude, this corresponds to a horizontal scanning by the radiometer over the surface of ~1 m. Taking a period of 100 s, the amplitude of the velocity of the scanning motion is 0.01 m s^{-1}, which is an order of magnitude less than typical surface drift velocities. We therefore conclude that the effects of the motion of *FLIP* on the low-frequency sea surface temperature spectra are negligible, even though the effects on coherence spectra are marginally significant at the 95% level.

Representative phase spectra computed for wave height and surface temperature are shown in Fig. 7. The phases at frequencies corresponding to the peak in the wave spectra are between zero and −30°, indicating that warm fluctuations in temperature are associated with the region just upwind of the crest of the dominant gravity waves. The cause of this behavior may be locally enhanced wind stress on the upwind side of the crest of the wave. This part of the wave profile is most favorably exposed to the wind. The increased wind stress could act directly to thin the viscous layer just beneath the surface (Saunders, 1967), thereby exposing the warmer water below, or the enhanced stress could generate a patch of capillary waves which could act to thin the viscous layer, as suggested by Witting (1971).

As shown in Fig. 7, when frequency increases from 0.05 to 0.5 Hz, the phase between the surface temperature and wave height increases from between zero and −30° to about 100°, i.e., warm fluctuations occur on the downwind faces of the shorter period gravity waves. The downwind side of the wave profile has the greatest slope and is therefore the most unstable. It is also a region in which there is local convergence at the surface which tends to increase the amplitude of the capillary waves, giving rise to the possibility of thinning the viscous layer, as suggested by Witting (1971). There are warm spikes in the records of surface temperature shown in Fig. 3 which are associated with the steep downwind slopes of the waves.

All of the coherence and phase spectra are shown in Figs. 8 and 9, respectively, together with the averaged spectra. The characteristics are very similar to those in the representative spectra. There is a maximum in the coherence of 0.5 at 0.1 Hz. The mean phase is about −30° at a frequency corresponding to peaks in the wave spectra, and increases to about 100° at 0.4 Hz. As described above, the high values of coherence at low frequencies (0.01 Hz) are caused by the motion of *FLIP*.

5. Saunders' formula

An evaluation of the constant in Saunders' formula Eq. (1) was carried out. The mean differ-

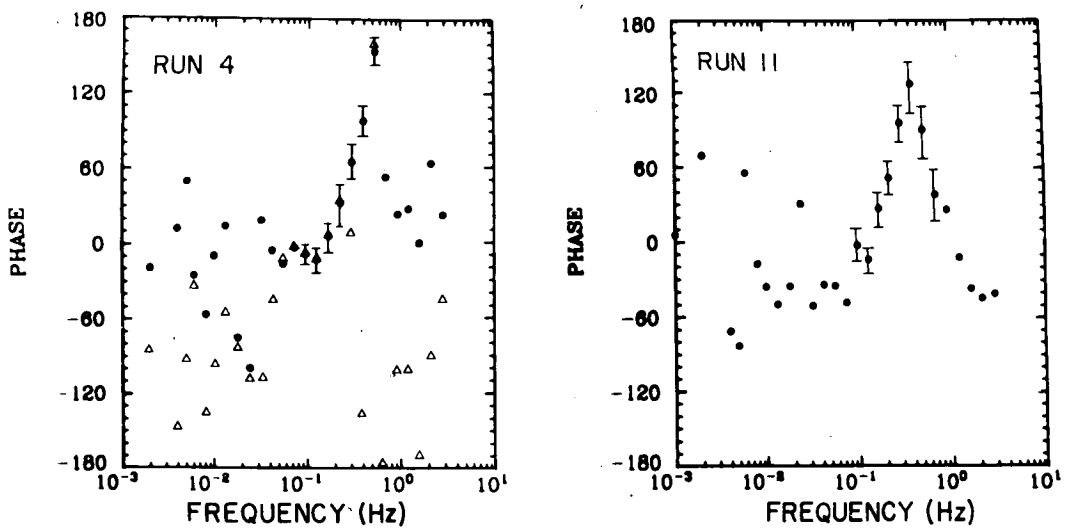

FIG. 7. Representative phase spectra for sea surface temperature and wave height (circles). A positive phase occurs when surface temperature leads wave height. The corresponding phase spectrum (run 4) for sea surface temperature and first differenced wave height ($\Delta\eta$) is shown by the triangles. The phase spectrum of (T_s,$\Delta\eta$) was recolored.

ence, $T_b - T_s$, between the surface temperature and the bulk temperature of the well-mixed water below was estimated by subdividing the surface temperature record for each run into intervals of 2 min. Within each interval, the maximum and mean surface temperatures were computed. The maximum difference between the mean and maximum values for the entire run was taken as an estimate of $T_b - T_s$. Implicit in the method is the assumption that at least once during each run the viscous sublayer below the surface viewed by the radiation thermometer is thinned so that the observed temperature is representative of the bulk, well-mixed water below. The record was subdivided into 2 min intervals to minimize the effects of trends in surface temperature. The values of $T_b - T_s$ computed as

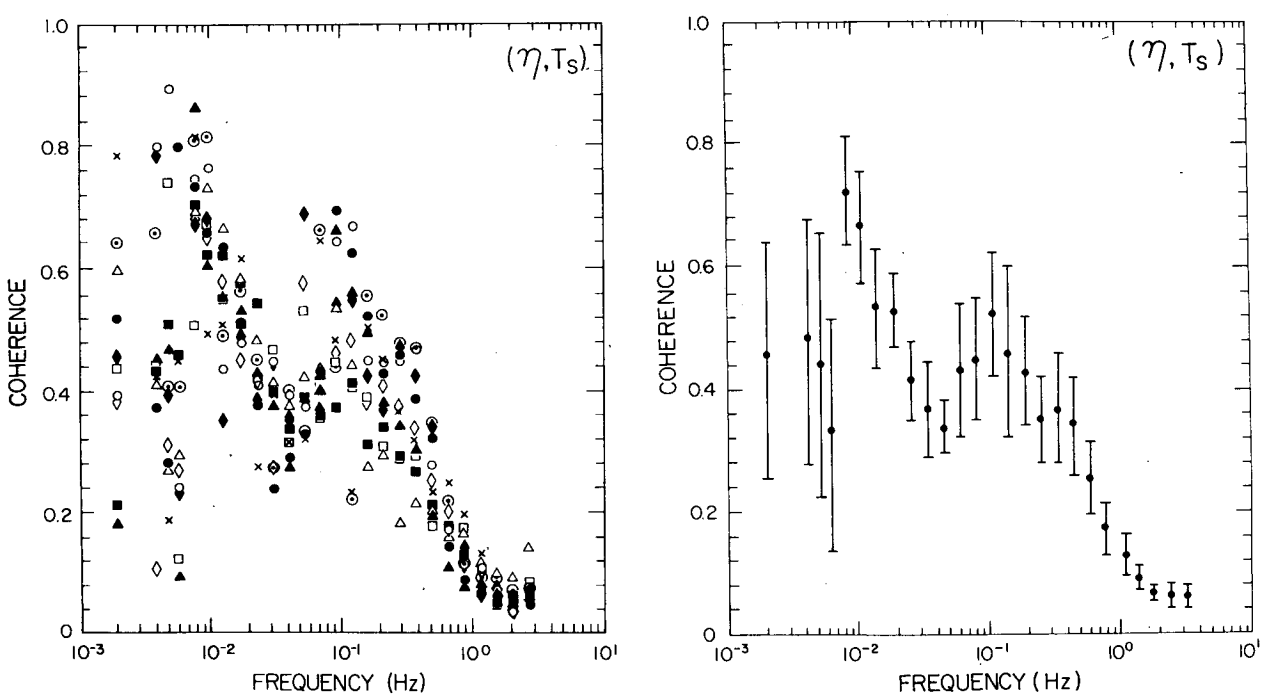

FIG. 8. Coherence spectra. Symbols are defined in Table 1. The average is over all runs.

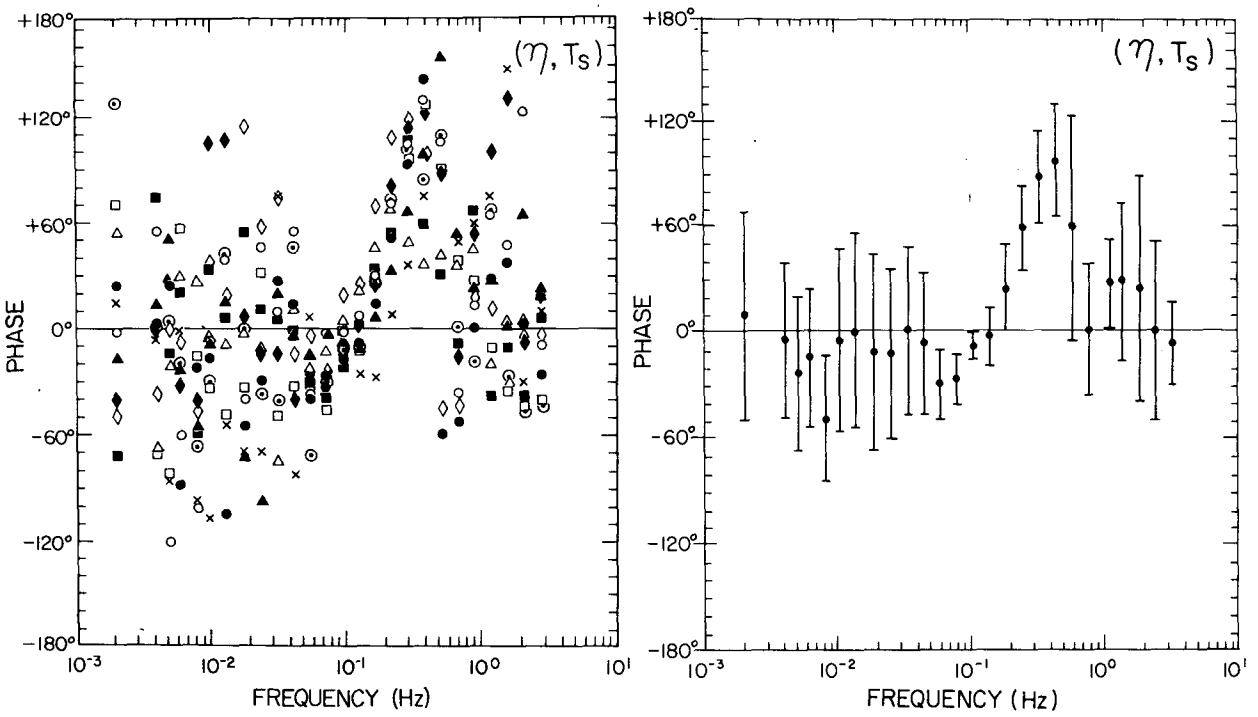

FIG. 9. Phase spectra. Symbols are defined in Table 1. The average is over all runs. Phase is defined as positive when surface temperature leads wave height.

described above are given in Table 1. Values of the dimensionless coefficient computed using Eq. (1) are also tabulated. The value of λ ranges from 5 to 9 with a mean of 7. This value is in good agreement with Saunders' (1967) suggested range of 5 to 10 and also agrees with Hasse's (1971) model and observations (Paulson and Parker, 1972) and with Deacon's (1977) model. Agreement is also good with observations over a cooling pond reported by Wesley (1979) who found $\lambda = 6$ at 15°C. He also found that λ was proportional to $Pr^{-1/3}$, where Pr is the Prandtl number. The agreement is less satisfactory with the value of $\lambda = 5$ determined by Grassl (1976) for a wind speed of 7 m s^{-1}. Grassl also suggests that λ varies with wind speed, increasing from $\lambda = 2$ at 1 m s^{-1} to $\lambda = 6$ at 10 m s^{-1}. Our observations are over too restricted a range of wind speed to draw any conclusions about a possible variation of λ. A plot of the left side of Eq. (1) vs $T_b - T_s$ is shown in Fig. 10.

The fact that the results reported here agree with the large body of observations reported by Hasse (1971), in which T_s was determined by extrapolating nearly adiabatic atmospheric temperature profiles to the surface, lends support to the method employed here. It was not possible to make an independent estimate of T_s and T_b in our case, because the absolute accuracy of the radiometrically determined temperatures was not adequate for reliable estimates of $T_b - T_s$. This is primarily because of the reflection of sky radiation and the impracticability of frequent calibration of the radiation thermometer as was done by Grassl (1976).

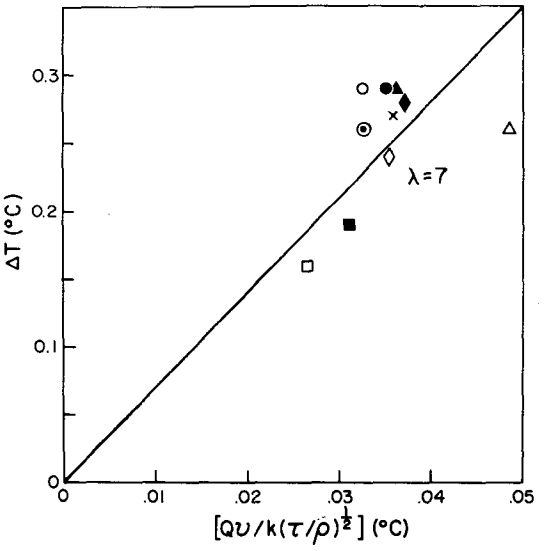

FIG. 10. The mean temperature difference ΔT between the surface and the well-mixed water below versus a quantity having dimensions of temperature where Q is the upward heat flux just below the interface, ν the kinematic viscosity of seawater, k the thermal conductivity, τ the surface stress and ρ the density of seawater. The line drawn represents Saunders' (1967) formula with $\lambda = 7$ (from Table 1).

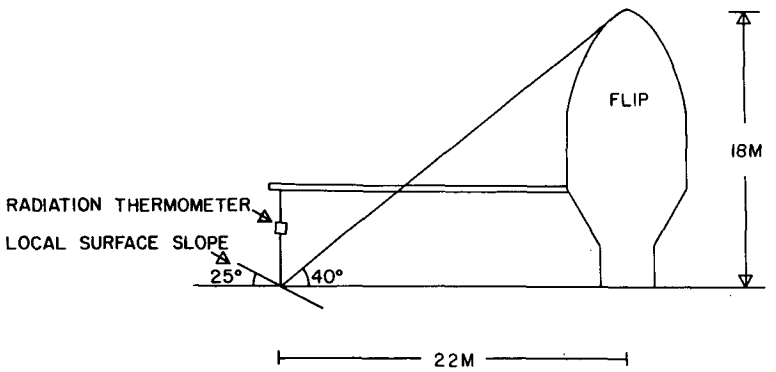

FIG. 11. Schematic diagram showing geometry associated with radiation coming from the hull of *FLIP* which is reflected into the radiation thermometer.

6. Conclusions

The following conclusions can be drawn:

1) Spectra of surface temperature over the sea exhibit a plateau between 0.05 and 0.5 Hz, followed by a rapid decrease in energy for frequencies above 1 Hz. There is usually a small peak in the temperature spectrum at the same frequency as the peak in the wave spectrum.

2) There is a peak in the coherence spectra between surface temperature and wave height occurring at the same frequency as the peak in the wave spectra. The average magnitude of the peak in coherence is 0.5.

3) The phase angle between wave height and surface temperature at the frequency of the peak in the wave spectrum is $-30°$ on average, indicating warm surface temperature upwind of the crests of the dominant gravity waves. The cause of these warm fluctuations is thought to be locally enhanced wind stress which thins the viscous layer just beneath the surface, either directly or through generation of capillary waves (Witting, 1971).

4) The phase spectrum between surface temperature and waves increases from an average of $-30°$ at 0.06 Hz to 100° at a frequency of 0.4 Hz. The phase relation at 0.4 Hz implies that warm temperature fluctuations are associated with the steep portion of gravity waves downwind from the crest. The cause of the warm fluctuations may be due to the generation of turbulence in the water caused by instability of the surface or may be due to the enhancement of the amplitude of capillary waves caused by convergence of the surface. Both of these effects would tend to thin the viscous layer just below the surface, exposing warmer water from below.

5) On the basis of the observations of mean values of $T_b - T_s$ inferred from surface temperature fluctuations, the constant in Saunders' (1967) formula [Eq. (1)] is $\lambda = 7$. This value is in fair agreement with other determinations over the ocean which range from 5 to 8. It is perhaps surprising that the observations also agree with models of Hasse (1971) and Deacon (1977) which are based on laboratory observations of flow near solid boundaries. These models are similar to Saunders' formula, but they contain no arbitrary constants. This suggests that the effects of waves in determining ΔT may be small or compensating.

Acknowledgments. This research was supported by the Office of Naval Research. The cooperation of the officers and crew of the R/P *FLIP* and the assistance of A. Lillich in carrying out part of the analysis is gratefully acknowledged. Some of the computations were carried out at the computer facility of the National Center for Atmospheric Research, which is sponsored by the National Science Foundation. The typing assistance of Ruth Ebey, Sue Watt, Wanda Brown and Sharon McBride contributed greatly to the timely completion of this work. The figures were prepared by the MLRG graphics group at Scripps under the direction of Fred Crowe.

APPENDIX

Effect of Reflections on Measurement of Surface Temperature

The objective of this Appendix is to evaluate possible errors in the radiometric measurements of sea surface temperature caused by reflections of longwave radiation emanating from the hull of *FLIP*, the boom and supports, and from the radiation thermometer itself. These reflections are a possible source of error because the emitting surfaces are generally much warmer than the sky, the only remaining source of reflected longwave radiation at night. The errors are evaluated by use of simple models.

We first consider radiation reflected from the hull of *FLIP*. From Fig. 11 it is apparent that only waves sloping toward the hull can reflect radiation from the

hull into the radiometer. The height of the hull above the water is about 18 m and the horizontal distance from the centerline to the radiation thermometer is 22 m. The angles between the rays coming from the hull and the horizontal must therefore be less than $40° = \tan^{-1}(18/22)$. Snell's law states that the angle of incidence is equal to the angle of reflection. Consider a ray 40° from the horizontal arriving just below the radiation thermometer. The water surface below the instrument must be inclined toward the direction from which the ray is coming by an angle 25° from the horizontal for this ray to be reflected vertically into the instrument (Fig. 11). Radiation from the hull will be reflected into the instrument only when the water surface below the hull is inclined at an angle > 25° toward the hull.

According to Stokes (Kinsman, 1965, p. 19), the steepest gravity waves have a steepness (ratio of wave height to wavelength) of 1/7. A sinusoidal wave having a steepness of 1/7 has a maximum slope of $\pi/7$, corresponding to an angle with the horizontal of 24°. Thus, according to this criterion, we would expect negligible radiation from the hull to be reflected into the radiometer.

This conclusion is supported by other evidence. Cox and Munk (1954) observed that the probability distribution of surface slopes was approximately Gaussian with rms surface slope less than tan 16° for wind speeds less than 14 m s^{-1}. Slopes greater than 24° have a probability for winds at 10 m s^{-1} of ~0.01. Slopes greater than 24° oriented to reflect radiation from the hull into the instrument have a probability less than 0.001.

We next consider the reflection of radiation emanating from the boom. We consider the simplest case with the water surface horizontal as shown schematically in Fig. 12. The radius, r_{bm} of the disc on the boom emitting radiation which is reflected into the radiation thermometer is

$$r_{bm} = (h_1 + h_2)\tan(\alpha/2),$$

where α is the angular field of view of the instrument (2°). Assuming that the longwave radiation is emitted isotropically, the radiative flux density on an arc of radius h_1 whose origin coincides with the center of the disc on the boom is

$$\sigma T_{bm}^4 (r_{bm}^2/h_1^2)\cos\theta,$$

where r_{bm} is the radius of the disc on the boom and θ the angle between h_1 and the normal to the disc on the boom. Therefore, the radiative flux arriving from the boom which is reflected into the radiometer is

$$\Gamma\sigma T_{bm}^4 (r_{bm}^2/h_1^2)\pi r_s^2,$$

where Γ is the reflectivity of the surface for longwave radiation, taken equal to 0.02, σ the Stefan-Boltzman constant and r_s the radius of the disc on the surface viewed by the radiation thermometer. We may then write

$$T_{sm}^4 = T_s^4 + \Gamma T_{bm}^4 (r_{bm}^2/h_1^2)\pi r_s^2,$$

where T_{sm} is the surface temperature measured by the radiometer, T_s is the true surface temperature, and we have assumed that reflected radiation from the boom is the only source of error. In estimating the error we take $T_{bm} = T_s$ because at night the boom is never colder than the dew point, which was never more than 2°C less than the surface temperature. Substituting numerical values we find that

$$T_{sm}/T_s = 1 + 4 \times 10^{-8}.$$

Taking $T_s = 287$ K, the mean for the experiment, the error is 5×10^{-5} °C which is certainly negligible in comparison to the magnitudes of the observed fluctuations in T_s and is also far below the resolution of the instrument.

We might also have considered the error due to reflected radiation from the radiation thermometer itself. It is clear that the error induced would be similarly negligible.

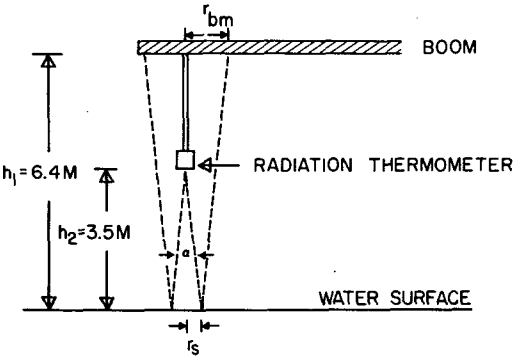

FIG. 12. Schematic diagram showing reflection of longwave radiation from the boom into the radiation thermometer.

REFERENCES

Amos, D. E., and L. H. Koopmans, 1963: Tables of the distribution of the coefficient of coherence for stationary bivariate Gaussian processes. Sandia Corp., Monograph SCR-483, 328 pp.

Ball, F. K., 1954: Sea surface temperatures. *Aust. J. Phys.*, **7**, 649–652.

Bendat, J. S., and A. G. Piersol, 1971: *Random Data: Analysis and Measurement Procedures*. Wiley-Interscience, 407 pp.

Blackman, R. B., and J. W. Tukey, 1958: *The Measurement of Power Spectra from the Point of View of Communications Engineering*. Dover, 190 pp.

Bronson, E. D., and E. R. Glosten, 1968: Floating Instrument Platform. Scripps Institute of Oceanography, University of California, Mar. Phys. Lab. Tech. Rep., SIO Ref. No. 62-24, 23 pp.

Cooley, J. W., P. A. W. Lewis and P. D. Welch, 1967: The fast Fourier transform algorithm and its applications. Tech. Rep. RC 1743, IBM Watson Research Center, Yorktown Heights, NY, 157 pp.

Cox, C. S., and W. Munk, 1954: Statistics of the sea surface derived from sun glitter. *J. Mar. Res.*, **13,** 198–227.

Deacon, E. L., 1977: Gas transfer to and across an air-water interface. *Tellus,* **29,** 363–374.

Ewing, G., and E. D. McAlister, 1960: On the thermal boundary layer of the ocean. *Science,* **131,** 1374–1376.

Grassl, H., 1976: The dependence of the measured cool skin of the ocean on wind stress and total heat flux. *Bound.-Layer Meteor.*, **10,** 465–474.

Hasse, L., 1971: The sea surface temperature deviation and the heat flow at the sea-air interface. *Bound.-Layer Meteor.*, **1,** 368–379.

Hill, R. H., 1972: Laboratory measurement of heat transfer and thermal structure near an air-water interface. *J. Phys. Oceanogr.*, **2,** 190–198.

Jenkins, G. M., and D. G. Watt, 1968: *Spectral Analysis and Its Applications.* Holden-Day, 523 pp.

Julian, P. R., 1974: Comments on the determination of significance levels of the coherence statistics. *J. Atmos. Sci.*, **32,** 836–837.

Kinsman, B., 1965: *Wind Waves; Their Generation and Propagation on the Ocean Surface.* Prentice-Hall, 676 pp.

McAlister, E. D., 1964: Infrared optical techniques applied to oceanography, 1, Measurement of total heat flow from the sea surface. *Appl. Opt.*, **3,** 609–612.

——, and W. McLeish, 1969: Heat transfer in the top millimeter of the ocean. *J. Geophys. Res.*, **74,** 3408–3414.

Miller, A. W., Jr., and R. L. Street, 1978: On the existence of temperature waves at a wavy air-water interface. *J. Geophys. Res.*, **83,** 1353–1365.

Panofsky, H., and G. Brier, 1958: *Some Applications of Statistics to Meteorology.* The Pennsylvania State University Press, 224 pp.

Paulson, C. A., and T. W. Parker, 1972: Cooling of a water surface by evaporation, radiation and heat transfer. *J. Geophys. Res.*, **77,** 491–495.

Saunders, P. M., 1967: The temperature at the ocean-air interface. *J. Atmos. Sci.*, **24,** 269–273.

——, 1970: Corrections for airborne radiation thermometry. *J. Geophys. Res.*, **75,** 7596–7601.

Weseley, M. S., 1979: Heat transfer through the thermal skin of a cooling pond with waves. *J. Geophys. Res.*, **84,** 3696–3700.

Witting, J., 1971: Effects of plane progressive irrotational waves on thermal boundary layers. *J. Fluid Mech.*, **50,** 321–324.

Woodcock, A. H., 1941: Surface cooling and streaming in shallow, fresh and salt waters. *J. Mar. Res.*, **4,** 153–161.